



Climatic limit for agriculture in Brazil

Ludmila Rattis ^{1,2}✉, Paulo M. Brando ^{1,2,3}, Marcia N. Macedo ^{1,2}, Stephanie A. Spera ⁴, Andrea D. A. Castanho ¹, Eduardo Q. Marques ⁵, Nathane Q. Costa ², Divino V. Silverio ⁶ and Michael T. Coe ^{1,2}

Brazil's leadership in soybean and maize production depends on predictable rainfall in the Amazon-Cerrado agricultural frontier. Here we assess whether agricultural expansion and intensification in the region are approaching a climatic limit to rainfed production. We show that yields decline in years with unusually low rainfall or high aridity during the early stages of crop development—a pattern observed in rainfed and irrigated areas alike. Although agricultural expansion and intensification have increased over time, dry-hot weather during drought events has slowed their rate of growth. Recent regional warming and drying already have pushed 28% of current agricultural lands out of their optimum climate space. We project that 51% of the region's agriculture will move out of that climate space by 2030 and 74% by 2060. Although agronomic adaptation strategies may relieve some of these impacts, maintaining native vegetation is a critical part of the solution for stabilizing the regional climate.

Over the past four decades, Brazil's agriculture sector has invested in innovation, technical assistance, public loans and agricultural intensification—all of which have contributed to increasing grain production. Brazil now produces 32% of the world's soybeans and 8% of its maize¹, with agribusiness representing ~21% of the country's gross domestic product² in 2019. The Amazon-Cerrado region (ACR) is among the world's largest agricultural regions³, responsible for half of Brazil's agricultural output today and expected to increase by 30% in the next decade⁴. Despite its meteoric growth, Brazil's agricultural system also faces substantial risks because it depends on a stable climate to sustain crop production. With ~90% of its cropped area in rainfed production⁵, agriculture in the ACR is highly vulnerable to droughts, heat-waves and other climatic disruptions⁶.

Climate change—influenced by global heating and deforestation-related disruptions to the hydrological cycle^{7,8}—could stymie Brazil's ambitions to increase crop production. De-intensification (that is, fallowing or shifting from double to single cropping⁹) and declining crop yields will probably follow projected regional increases in air temperature¹⁰, air dryness^{11,12}, drought frequency and intensity, and dry-season length¹³. Recent droughts in the ACR offer important insights into how Brazil's agricultural frontier may respond to such climate changes. Failure to adapt could have important adverse effects on global food systems, given that Brazil produces a large fraction of the world's soybeans and maize^{3,14}.

In this Article, we investigate the climatic sensitivity of agriculture in the states of Mato Grosso, Goiás, Maranhão, Tocantins, Piauí and Bahia (the latter four comprising the MATOPIBA region¹⁵; Fig. 1 and Extended Data Fig. 1), where half of all Brazilian crops are grown. We focus on three key questions: (1) Have recent droughts influenced the rate of agricultural intensification, de-intensification or agricultural yields? (2) Has recent expansion/intensification of agriculture occurred in regions vulnerable to climate changes? (3) To what extent have climate changes already affected agricultural suitability, and how is that projected to change in the near term?

Trends in cropland expansion

Since the early 2000s, agriculture has expanded to a broad swath of the savannah–rainforest transition zone (Fig. 1a–f). Compared with the long-term average (Methods), this expansion occurred in areas with similar rainfall and higher vapour pressure deficit (VPD, a proxy for atmospheric water demand; Fig. 1a–c), two important predictors of crop yield^{16,17}. A total of 76,072 km² of new agricultural land was added during 2001–2016 (Supplementary Table 1), which can be divided into three phases. In the first phase (2002–2006), 27,380 km² of cropland expanded into new areas with an average growing-season rainfall of 1,540 mm and growing-season VPD of 1.33 kPa. Although average precipitation was comparable to previous decades, the average VPD in areas added during 2002–2006 was above the optimal range for soybeans (~2.0 kPa (ref. ^{18,19})) and below that for maize (~1.7 kPa (ref. ²⁰)), when water stress starts to severely compromise maize yield; Supplementary Fig. 1). During the second phase (2007–2011), 18,722 km² of cropland expanded into regions characterized by lower precipitation and higher growing-season dryness (mean precipitation: 1,525 mm, VPD: 1.41 kPa) compared with the long-term average. In the past expansion phase (2012–2016), 29,970 km² of new agriculture expanded into areas with higher precipitation (1,588 mm in the growing season) than the long-term average and higher VPD (1.39 kPa) compared with the first phase.

Drought effects on agricultural yield

Our analyses show that droughts decreased crop yields for both rainfed and irrigated systems (Fig. 2). In rainfed areas, soybeans experienced modest production losses during droughts (-5 kg ha^{-1} and -26 kg ha^{-1} in the Cerrado biome and Mato Grosso state, respectively), whereas the maize second crop experienced substantial losses ($-1,353 \text{ kg ha}^{-1}$ and -892 kg ha^{-1}). For municipalities with some irrigation, we observed much lower soybean yields during droughts compared with municipalities without irrigation, probably because regions with irrigation are generally drier (Supplementary

¹Woodwell Climate Research Center, Falmouth, MA, USA. ²Instituto de Pesquisa Ambiental da Amazônia, Canarana, Brazil. ³Department of Earth System Science, University of California Irvine, Irvine, CA, USA. ⁴Department of Geography and the Environment, University of Richmond, Richmond, VA, USA. ⁵Universidade do Estado do Mato Grosso, Nova Xavantina, Brazil. ⁶Universidade Federal Rural da Amazônia, Capitão Poço, Brazil.

✉e-mail: lrattis@woodwellclimate.org

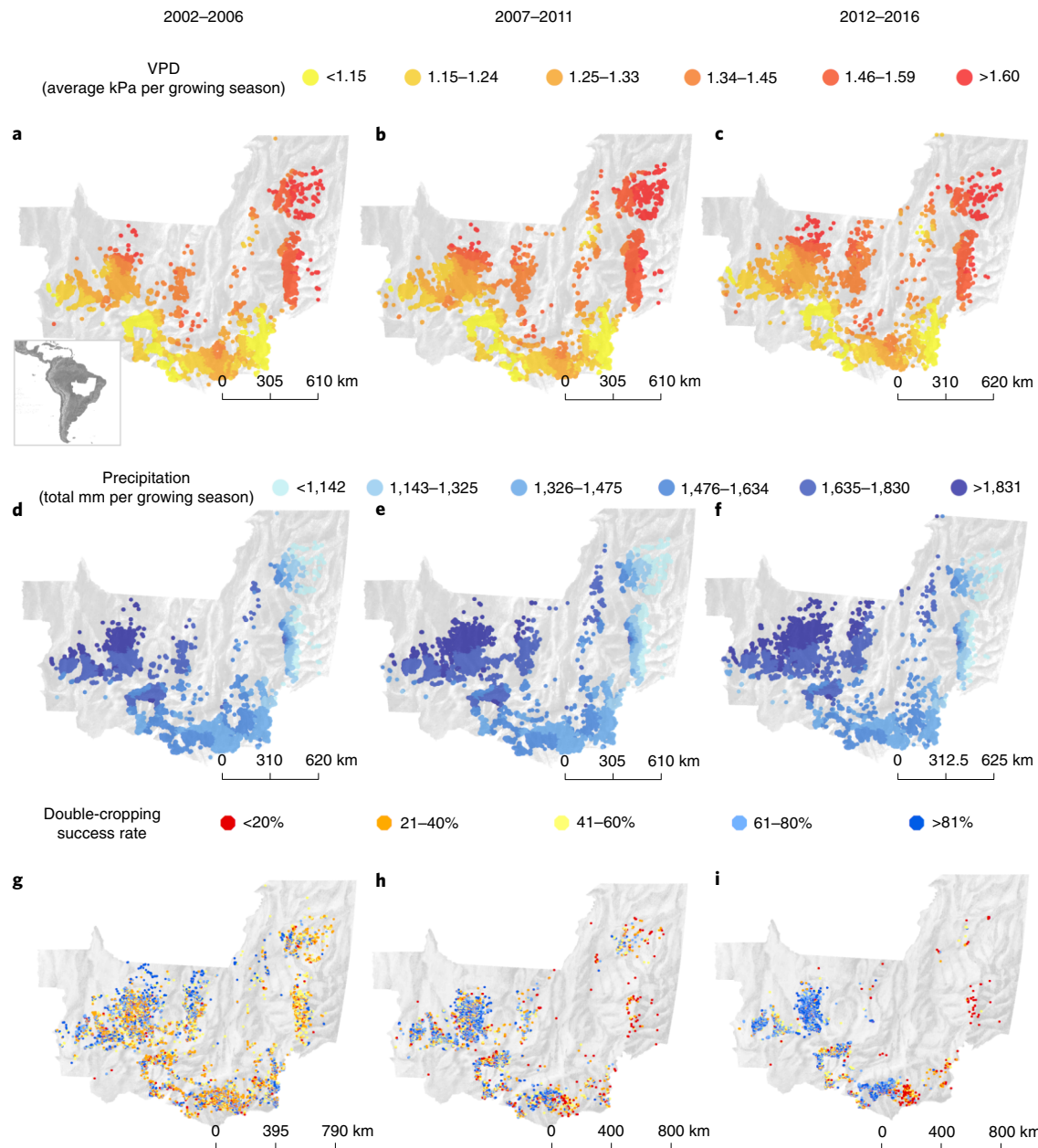


Fig. 1 | The historical distribution of agricultural fields and climate variables in the ACR. The ACR includes parts of midwestern, northern and northeastern Brazil, including the states of Mato Grosso, Goiás, the Federal District of Brasília and Tocantins and western Bahia, southwestern Piauí and southern Maranhão. **a–c**, VPD for the newly expanded areas in each period during the growing season. **d–f**, Precipitation for each period, also just for the newly expanded agriculture areas, during the growing season. **g–i**, Double-cropping intensity or success rate (fraction), defined as the number of years when double cropping occurred divided by the total number of years in each of the three periods: 2002–2006 (**a,d,g**), 2007–2011 (**b,e,h**) and 2012–2016 (**c,f,i**). Cool colours represent higher cropping intensity; warm colours represent lower cropping intensity.

Table 2; Cerrado: -142 kg ha^{-1} ; Mato Grosso: -111 kg ha^{-1}). In contrast, irrigation apparently mitigated losses in maize yield during droughts, though more in the Cerrado (absolute loss of -24 kg ha^{-1}) than in Mato Grosso (-665 kg ha^{-1}).

In general, monthly precipitation and VPD variations explained a large portion of the variability in historical yields for soybeans (1988–2019) and maize second crop (2003–2019). Together, they explained 39% (Cerrado) and 48% (Mato Grosso) of soybean yield variability and 19% (Cerrado) and 52% (Mato Grosso) of maize second-crop yield variability (Extended Data Fig. 2). Statistical models including VPD and precipitation during the early growing period

ranked highest in explaining the yield variability of soybeans and maize. A sensitivity analysis for Mato Grosso showed that (assuming mean rainfall: 230 mm per month) for each 1.0 kPa increase in growing-season VPD, soybean yields decreased by 48 kg ha^{-1} (95% confidence interval ($\text{CI}_{95\%}$) = -88 kg ha^{-1} to -9 kg ha^{-1}) in non-drought years and by 152 kg ha^{-1} ($\text{CI}_{95\%}$ = -197 kg ha^{-1} to -107 kg ha^{-1}) during droughts. The same analysis for the Cerrado showed that (assuming mean precipitation: 180 mm per month) for each 1.0 kPa increase in growing-season VPD, soybean yields decreased by 50 kg ha^{-1} ($\text{CI}_{95\%}$ = -64 kg ha^{-1} to -35 kg ha^{-1}) in non-drought years and by 106 kg ha^{-1} ($\text{CI}_{95\%}$ = -126 kg ha^{-1} to

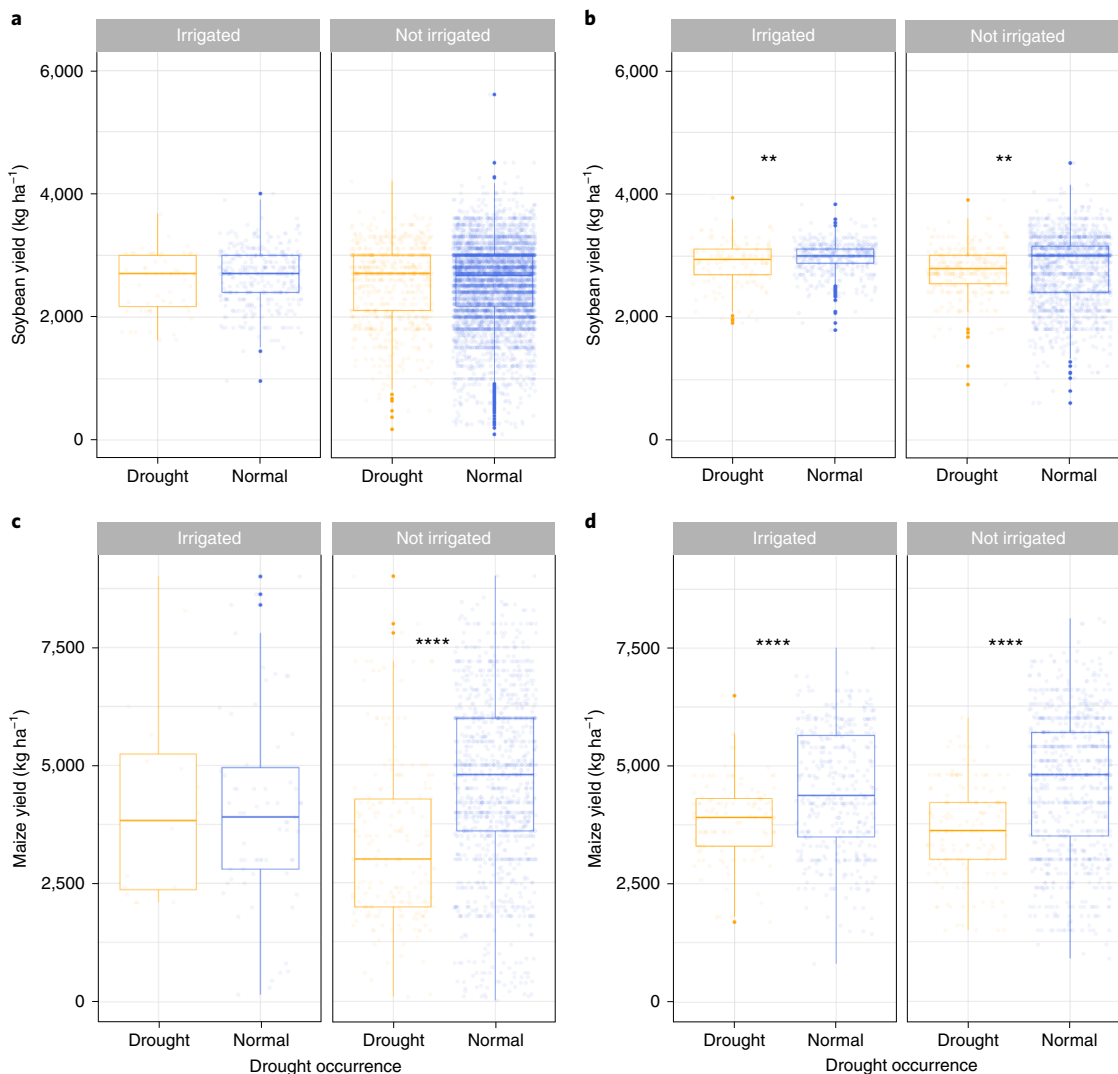


Fig. 2 | Soybean and maize yields for Mato Grosso and the Cerrado under normal and dry conditions and under rainfed and irrigated management.

a-d, Soybean ($n=664$) (**a,b**) and maize second-crop ($n=654$) (**c,d**) yields reported by IBGE from 1988 to 2019 for soybean and from 2003 to 2019 for maize second crop. The municipalities located in Maranhão, Tocantins, Piauí, Bahia and Goiás were considered here as the Cerrado region (**a,c**), and municipalities located in Mato Grosso, mostly within the Brazilian Legal Amazon (**b,d**). Municipalities with a reported occurrence of irrigation⁵ were grouped as 'irrigated', whereas the others were grouped as 'not irrigated'. Drought occurrence is based on described years of intense and widespread drought in the region according to the literature. Years of drought in the Cerrado region: 1984–1985, 1990–1991, 2007–2008 and 2015–2016. Years of drought in Mato Grosso state: 1997–1998, 2005–2006, 2010–2011 and 2015–2016. Absolute numbers represented in the box plots are available in Supplementary Table 2. Asterisks indicate significant difference between medians.

$\sim 86 \text{ kg ha}^{-1}$) during droughts. Early growing-season climate variations had no clear effect on maize yields in Mato Grosso (-13 kg ha^{-1} , $\text{CI}_{95\%} = -103 \text{ kg ha}^{-1}$ to 77 kg ha^{-1}) or the Cerrado (-132 kg ha^{-1} , $\text{CI}_{95\%} = -399 \text{ kg ha}^{-1}$ to 135 kg ha^{-1}) in non-drought years. During droughts, however, our models projected maize yields in Mato Grosso to decrease by 825 kg ha^{-1} ($\text{CI}_{95\%} = -950 \text{ kg ha}^{-1}$ to -699 kg ha^{-1}) for each 1.0 kPa increase in VPD during the early growing season. In the Cerrado, our models show that maize yields decreased by 994 kg ha^{-1} ($\text{CI}_{95\%} = -1,188 \text{ kg ha}^{-1}$ to -801 kg ha^{-1}) for each 1.0 kPa in VPD in the early growing season. Hence, climate variability during the early stages of plant development is a critical determinant of crop yields, even in years that do not meet the statistical thresholds typically used to define drought conditions.

Drought effects on agricultural intensification

Intensive industrial agriculture (for example, double cropping) has expanded over time across the ACR (Fig. 3a). From 2001 to 2016,

we observed an $\sim 3,334 \text{ km}^2 \text{ yr}^{-1}$ average increase in the area planted with two crops per growing season (Supplementary Table 3 and Fig. 3a). The total double-cropped area increased nearly tenfold from $8,409 \text{ km}^2$ in 2001 to nearly $80,000 \text{ km}^2$ in 2014 before falling to $61,855 \text{ km}^2$ in 2016. Over the same period, the area planted with only one crop per growing season decreased from $51,824 \text{ km}^2$ in 2001 to $34,191 \text{ km}^2$ in 2016. The total double-cropped area surpassed the area in single cropping by 2012 and has remained higher ever since.

Despite a clear trend towards increased double cropping across the ACR, there was high spatial and temporal variability in cropping frequency—the number of crops during a single growing season. Double cropping was most consistently attempted (occurring in $>80\%$ of years) in central Mato Grosso and western Goiás (Fig. 1g–i). In contrast, it was attempted in less than 40% of years in southeastern Goiás and across the MATOPIBA region, where more extreme climate limited the ability to double crop—particularly in the later period (2012–2016), when it was rarely attempted.

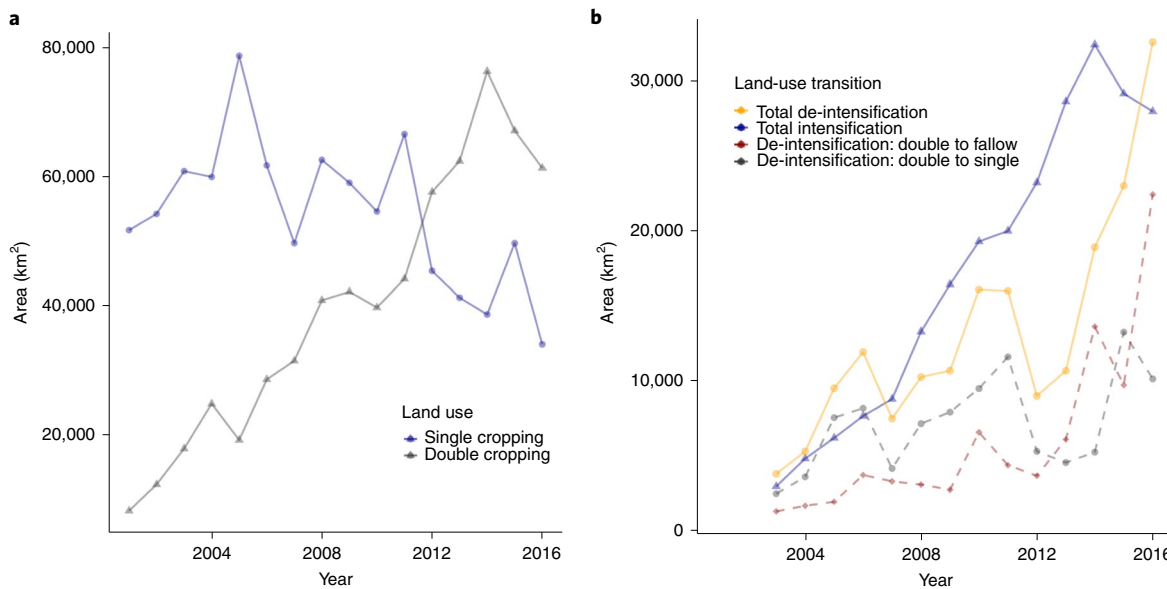


Fig. 3 | Land-use transition within the study area. **a**, Annual sum of land area (km^2) under double cropping (grey) and single cropping (blue) from 2001 to 2016. **b**, Total area of agriculture de-intensification (yellow), which is the sum of double cropping to fallow (red) and double to single cropping (grey). Total intensification (blue) represents the area moving from single to double cropping annually from 2003 to 2016. Land-use transition analysis started in 2003 because, in each case, we considered a two-year temporal filter to define the transitions. For the intensification trend analysis, just the pixels where land-use transition occurred were analysed. Agriculture intensification: $n = 360,004$; de-intensification: $n = 361,823$.

(Fig. 1). Agriculture transitioned from single to double crops at a steady rate of $2,349 \text{ km}^2 \text{ yr}^{-1} \pm 153 \text{ km}^2 \text{ yr}^{-1}$, increasing from about $3,000 \text{ km}^2 \text{ yr}^{-1}$ in 2003 to more than $30,000 \text{ km}^2 \text{ yr}^{-1}$ in 2014 (Fig. 3b). At the same time, every place where double cropping was attempted (Methods) transitioned back to single cropping at least once during the study period. This de-intensification process increased from $\sim 3,000 \text{ km}^2 \text{ yr}^{-1}$ in 2003 to $\sim 10,000 \text{ km}^2 \text{ yr}^{-1}$ in 2012, followed by a rapid increase thereafter (Fig. 3). By 2016, more than $32,000 \text{ km}^2$ had temporarily shifted back to less-intensive agriculture, about $4,616 \text{ km}^2$ greater than the amount shifting to double cropping that year. These results show that the probability of agricultural areas transitioning from double to single cropping (or fallow) has increased over time.

De-intensification of the cropping system was more likely to occur in drought years and in areas with sandy soils (Extended Data Fig. 3). Drought years were correlated with higher rates of transition from double to single cropping and from single cropping to fallow fields (that is, de-intensification; Fig. 3b). For example, during the droughts of 2005–2006, 2010–2011 and 2015–2016, we observed de-intensification of $11,933 \text{ km}^2$, $16,095 \text{ km}^2$ and $32,564 \text{ km}^2$, respectively (Figs. 1g–j and 3b). The areas shifting to less-intense agriculture were associated with below-average rainfall (fallow lands: -6% ; double to single cropping: -6%) and higher VPD (fallow lands: $+17\%$; double to single cropping: $+4\%$) compared with areas intensifying from single to double cropping (Supplementary Fig. 2). For each 100-mm decrease in total precipitation, the probability of double cropping decreased by 3.6% . Likewise, for each 1 kPa increase in VPD, the probability of double cropping decreased by 30% (Extended Data Fig. 4 and Supplementary Table 4; $R^2 = 0.14$). The areas undergoing de-intensification also exhibited poorer soil characteristics, including lower soil carbon, lower clay content and higher sand content. Finally, the onset of the growing (rainy) season tended to be delayed in areas that de-intensified (fallow lands: $+25\%$; double to single cropping: $+24\%$). Overall, these results point to agricultural intensification and expansion having occurred in areas with marginal²¹ climate and soils, which ultimately increased the probability of crop failure during drought years.

Changes in climate space of the ACR

To quantify how climate has changed historically and may change in the future, we used a set of climate variables to delineate the ‘climate space’ of agriculture, defined here by the relationship between growing-season water availability (precipitation) and water deficit (WD). In the 1970s, agricultural land in the ACR had a climate space with average rainfall of $1,579 \text{ mm}$ and a WD of -323 mm during the growing season (September to June; Fig. 1). Since the 1970s, the climate space over existing croplands in the ACR has become substantially warmer (primarily) and drier (secondarily; Fig. 4). Overall, across the ACR, average precipitation decreased by -19 mm and WD increased by $+150 \text{ mm}$. As a result, $26,551 \text{ km}^2$ of agricultural lands—approximately 28% of all areas cultivated in 2016—are now in climate conditions notably outside the agricultural climate space defined in the 1970s (Fig. 4 and Supplementary Table 5). Considering precipitation and WD as two axes in a Cartesian plane, we calculated the direction and speed of change (that is, Euclidian distance) for each agricultural plot in a two-dimensional climate space. On average, climate has shifted towards drier/warmer conditions ($191^\circ \text{C} \pm 0.3^\circ \text{C}$) at a rate of $5.7 \text{ mm yr}^{-1} (\pm 0.05 \text{ mm yr}^{-1})$ from 1970 to 2019 (Fig. 5).

Future climate projections point to much of the ACR agricultural land moving out of the most favourable climate space for rainfed agriculture (that is, the climate space where agriculture developed from the 1970s to the 1990s). Under an intermediate climate scenario (representative concentration pathway (RCP) 4.5 W m^{-2}), 51.5% ($49,506 \text{ km}^2$; Supplementary Table 5) of the current agricultural area would move outside the optimum climate space for rainfed agriculture by the 2030s (on the basis of the decadal mean climate), given projected decreases in precipitation (-124 mm) and increases in WD ($+411 \text{ mm}$). By the 2060s, projected climate changes would reduce growing-season rainfall by -145 mm and WD by -594 mm (compared with the 1970s), with 74% ($71,105 \text{ km}^2$) of agricultural lands falling outside the optimum climate space for rainfed agriculture (Extended Data Fig. 5 and Supplementary Table 5). Under RCP 8.5 W m^{-2} , 59% of the current cultivated area ($56,387 \text{ km}^2$) would have a climate less suitable for agriculture by the 2030s, and 91%

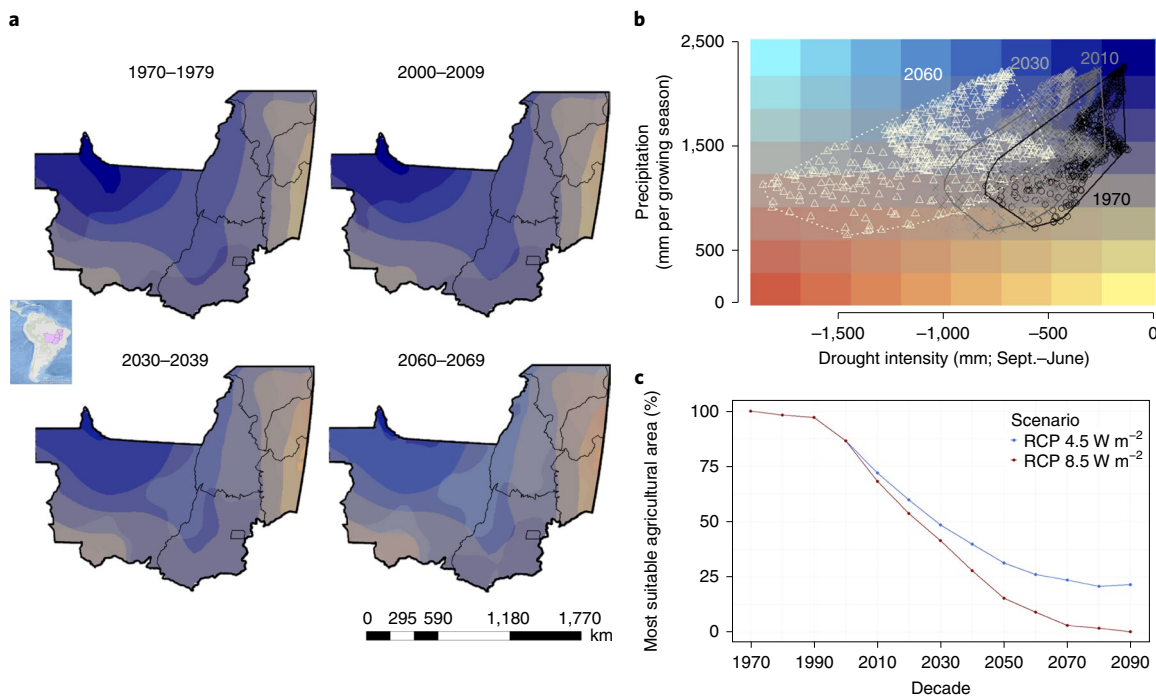


Fig. 4 | Mean climate space of the ACR over four decades. The historic climate space (1970–1979, 2000–2009) was defined using historical data, and the future climate space (2030–2039, 2060–2069) is based on the mean bias-corrected climate of 35 models taking part in CMIP5, scenario RCP 8.5 W m^{-2} . **a**, Maps of the climate space distribution. Colours correspond to specific combinations of precipitation and WD (defined in **b**). **b**, Scatterplot of all agricultural areas ($n=503$) as a function of their location in climate space. Each point on the scatterplot corresponds to one pixel on the maps. The minimum convex hulls mathematically delimit the climate space that would be occupied by the current (spatial) location of croplands in any given decade. **c**, The total decadal mean cropland area (% relative to the initial area) falling within the ideal climate space defined by the 1970s climate (that is, the black convex hull in **b**).

by the 2060s. These changes would occur at a rate of 18.8 mm yr^{-1} for RCP 4.5 (average angle of the vector: 194°) and 38.1 mm yr^{-1} for RCP 8.5 (192° ; Fig. 5 and Extended Data Fig. 6). Such near-term changes in climate would be faster and more intense than any observed rate of historical change—nearly 1.5-times faster under RCP 4.5 and 3-times faster under RCP 8.5.

Our results show that dry-hot years have led to sharp reductions in crop yield since the 1980s. Although Brazilian agriculture has expanded and intensified in the past 40 years, increased air dryness and recent droughts have reversed some of this intensification²¹, especially in drier-than-normal years. In addition, regional warming and drying from 1980 to 2019 have pushed 28% of current croplands out of the ideal climate space for rainfed agriculture. Most of these negative impacts occurred in areas of recent agricultural expansion (for example, southeastern Goiás and the MATOPIBA region), where climate approaches the dry boundary of the ideal climate space, and the soil has suboptimal properties. Future climate change could shrink the land area within the ideal climate space by over 51% as early as the 2030s. Under RCP 8.5 projections, 100% of existing croplands would be outside the ACR's preferred rainfed climate space by the 2090s.

Although official Brazilian data³ show that crop yields and production have grown since the mid-1980s, our analyses suggest that warming (primarily) and drying (secondarily) already pose serious threats to that system. Double cropping has been attempted throughout the ACR^{8,22}, but recurring droughts and delays in the onset of the rainy season^{12,13} have hindered its success, especially outside central Mato Grosso²³ and western Goiás. Consequently, the average cropping frequency (that is, the proportion of years that a property is double cropped since the first attempt) has decreased, particularly in areas where it was established after 2010. Our results

suggest that intensive rainfed agriculture (that is, expansion and intensification) may be approaching its upper limit, confirming previous results reported for Mato Grosso²⁴.

We find that total annual rainfall alone is not the best criterion for selecting agricultural areas that are resilient to near-term climate changes. The greatest climate risk is associated with the increased length and intensity of the dry season (as represented by VPD and WD). Despite this, farmers generally base their decisions to expand primarily on rainfall isohyets, which represent long-term historical averages. Our results confirm that recent agricultural expansion has focused in areas with higher average annual rainfall. Those same areas have higher (and increasing) VPD, which greatly increases crop water demand²⁵ and has been shown to impact maize yields²⁶ (-27.5% per kPa (ref. ¹⁷)). Under normal conditions, moving to areas with higher average VPD would not affect soybean or maize yields dramatically (observed decreases of $4\text{--}5 \text{ kg ha}^{-1}$ for soybeans, none for maize). However, as droughts become more frequent, areas under higher average VPD (in this case, an increase of 0.08 kPa) could see decreases between 12 kg ha^{-1} (Mato Grosso) and 34 kg ha^{-1} (Cerrado) for soybeans and 87 kg ha^{-1} (Mato Grosso) and 80 kg ha^{-1} (Cerrado) for maize. Such an increase would also lower the double cropping probability by 2.5%.

Despite the clear climate risks to production²⁷, the Brazilian government has targeted precisely the most vulnerable region for future expansion of cultivated areas^{4,28,29} (Fig. 4). This is largely because its agricultural development projections are based on economic criteria that fail to account for ongoing and future climate changes. By considering only logistical constraints³⁰ (for example, soils, slope, proximity to ports or markets, credit lines), the current model of agricultural growth could be setting Brazil up for major losses in the coming decades. Barring a different agricultural model or strong

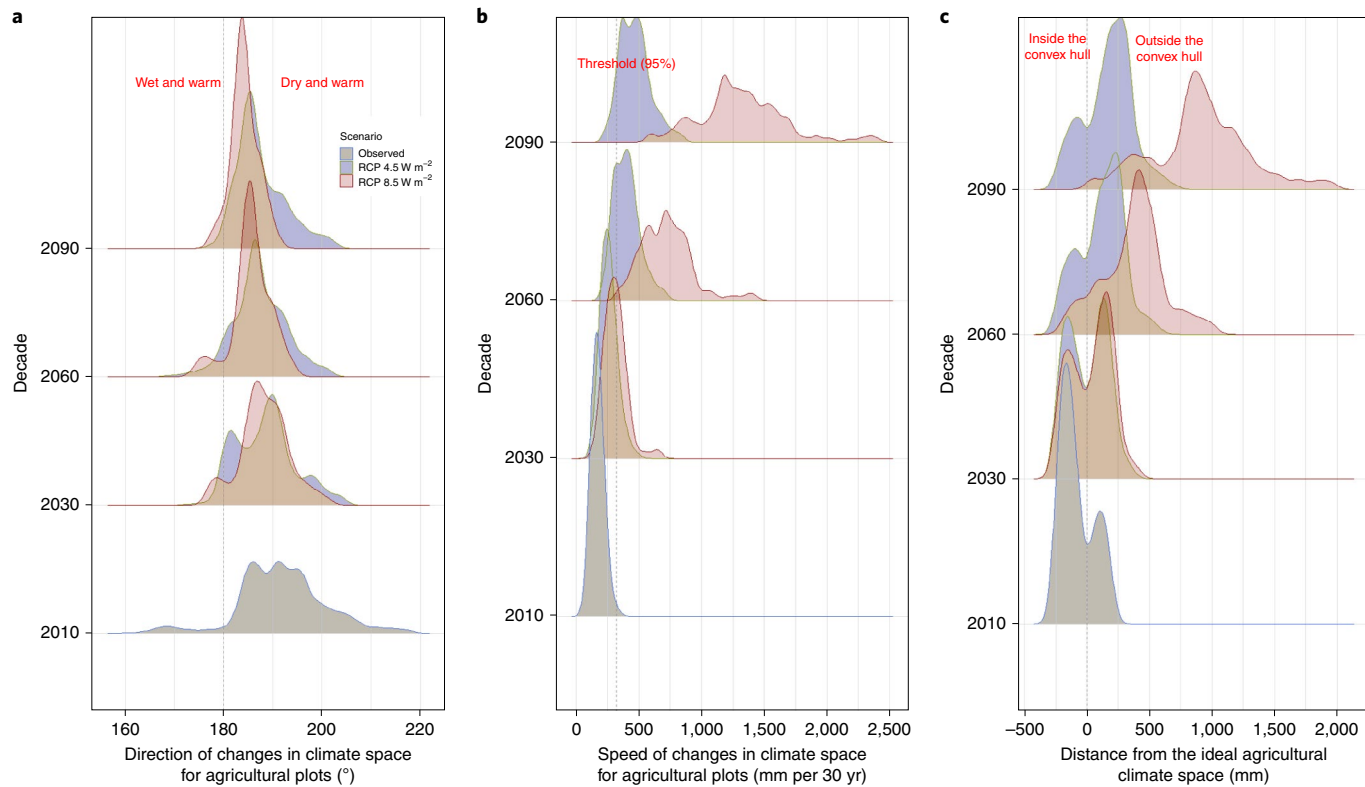


Fig. 5 | Projected changes in climate space associated with two RCPs of the IPCC. Considering precipitation and WD as two axes in a Cartesian plan, we calculated the direction, speed of change (that is, Euclidian distance) and climatological distance from the ideal agricultural climate spot for each agricultural plot in a two-dimensional climate space for two RCPs of the IPCC ($RCP 4.5 W m^{-2}$ and $RCP 8.5 W m^{-2}$). **a**, Predicted direction of change in climate space for today's agricultural fields (as in 2016; $n=503$). The dotted line indicates the climatic threshold for different directions of change: 90° to 180° indicates a shift towards wetter/warmer conditions; 180° to 270° indicates a shift towards drier/warmer conditions. **b**, Speed with which agricultural plots are expected to move in climate space over 30-year intervals. The dotted line indicates the threshold beyond which 95% of the points would travel outside the most favourable climate space for rainfed agriculture. **c**, Distance from the ideal climate space (dotted line). Both negative and positive values indicate the magnitude of the deviation from the ideal climate space, which is delineated by drawing a minimum convex hull around existing cropland pixels. On average, climate has shifted towards drier/warmer conditions ($191^\circ \pm 0.3^\circ$) at a rate of $5.7 mm yr^{-1} (\pm 0.05 mm yr^{-1})$ from 1970 to 2019.

adaptation strategies, Brazil's agricultural sector will probably face increasing crop losses from droughts, heatwaves and a lengthening dry season. Reducing these climate risks requires substantial research and investments in climate adaptation, some of which are already under way³⁰.

Evaluating irrigation potential. Although irrigation could remedy some of the climate changes described above, doing it at scale would require immense investments to expand energy production and distribution infrastructure³¹. The Brazilian government is now advocating for enormous irrigation expansion as a national priority⁵, but the trade-offs associated with these investments have yet to be fully evaluated. For example, large irrigation projects may lead to competition for water and energy between producers and urban areas³², exacerbating conflicts over these poorly managed resources³³. Such conflicts already exist in areas of recent, rapid irrigation expansion, such as western Bahia^{34,35}.

Developing drought-tolerant crop varieties. New cultivars could mitigate some of the projected losses associated with high VPD but may require translation of knowledge developed in temperate regions^{17,36} for application in the tropics. Moreover, historical strategies for plant genetic enhancement may already be hitting the yield ceiling^{37,38}. Brazil has succeeded in adapting cultivars to its varied edaphoclimatic conditions³⁹, but the unprecedented speed of climate change poses unexpected problems and exacerbates the

challenges inherent to tropical agriculture. Some yield losses (that is, from decreasing water-use efficiency) could be partially offset by CO_2 fertilization, but that would require finding germplasm capable of maintaining high water-use efficiency under novel climate conditions. For example, the positive effect of CO_2 fertilization has been shown to increase soybean yields by 32–47% up to a $\sim 2^\circ C$ increase above ambient temperature⁴⁰. However, recent studies indicate a 100% probability that Brazil will warm by over $4^\circ C$ before the end of the century⁴¹ under the current GHG emissions pathway^{42,43}. Under such harsh temperature conditions, crops in sandy soils will probably experience heat stress that overrides any potential gains from CO_2 fertilization.

Implementing climate-smart land and water management strategies. Maintaining forests and other native vegetation will be critical to help buffer regional climate in the near term. Native forests may improve crop yields by stabilizing regional temperature, VPD and rainfall and by modulating the length of the dry season^{7,10,13}. Thus, maintaining existing forests and reforesting where possible (or legally required) may help mitigate ongoing climate changes due to increasing atmospheric GHGs.

Our results show that droughts have already had important negative impacts on crop yields by changing the way temperature affects the early stages of plant development. Climate change may affect agricultural systems via several additional mechanisms that are beyond the scope of this study (Supplementary Information).

This study raises a potentially grave concern for the near future, as crop yield gains plateau and the area with suitable climate for crop production shrinks at an accelerating rate. Brazil is on a trajectory to have 70% of its croplands in the ACR with suboptimal climate in the next 30 years. Given that GHG emissions will probably continue, irrigation, cultivar development and forest conservation may be the only near-term options for avoiding catastrophic crop losses.

Online content

Any methods, additional references, Nature Research reporting summaries, source data, extended data, supplementary information, acknowledgements, peer review information; details of author contributions and competing interests; and statements of data and code availability are available at <https://doi.org/10.1038/s41558-021-01214-3>.

Received: 8 June 2020; Accepted: 8 October 2021;

Published online: 11 November 2021

References

1. Brazil. USDA Foreign Agricultural Service <https://www.fas.usda.gov/regions/brazil> (2019).
2. *Planilha do PIB do Agronegócio Brasileiro de 1996 a 2018* (Centro de Estudos Avançados em Economia Aplicada, 2018); <https://www.cepea.esalq.usp.br/br/pib-do-agronegocio-brasileiro.aspx>
3. Boletim da Safra de Grãos. *Companhia Nacional de Abastecimento* <https://www.conab.gov.br/info-agro/safra/graos/boletim-da-safra-de-graos> (2020).
4. *Projeções do Agronegócio: Brasil 2017/18 a 2027/28 Projeções de Longo Prazo* (Ministério da Agricultura, Pecuária e Abastecimento, 2018).
5. *Atlas Irrigação: Uso da Água na Agricultura Irrigada* (Agência Nacional de Águas, 2017).
6. Costa, M. H. et al. Climate risks to Amazon agriculture suggest a rationale to conserve local ecosystems. *Front. Ecol. Environ.* **17**, 584–590 (2019).
7. Fu, R. et al. Increased dry-season length over southern Amazonia in recent decades and its implication for future climate projection. *Proc. Natl Acad. Sci. USA* **110**, 18110–18115 (2013).
8. Spera, S. A., Galford, G. L., Coe, M. T., Macedo, M. N. & Mustard, J. F. Land-use change affects water recycling in Brazil's last agricultural frontier. *Glob. Change Biol.* **22**, 3405–3413 (2016).
9. Abrahão, G. M. & Costa, M. H. Evolution of rain and photoperiod limitations on the soybean growing season in Brazil: the rise (and possible fall) of double-cropping systems. *Agric. Meteorol.* **256–257**, 32–45 (2018).
10. Silvério, D. V. et al. Agricultural expansion dominates climate changes in southeastern Amazonia: the overlooked non-GHG forcing. *Environ. Res. Lett.* **10**, 104015 (2015).
11. Barkhodian, A., Saatchi, S. S., Behrang, A., Loikith, P. C. & Mechoso, C. R. A recent systematic increase in vapor pressure deficit over tropical South America. *Sci. Rep.* **9**, 15331 (2019).
12. Barkhodian, A., von Storch, H., Zorita, E., Loikith, P. C. & Mechoso, C. R. Observed warming over northern South America has an anthropogenic origin. *Clim. Dyn.* **51**, 1901–1914 (2018).
13. Leite-Filho, A. T., Costa, M. H. & Fu, R. The southern Amazon rainy season: the role of deforestation and its interactions with large-scale mechanisms. *Int. J. Climatol.* **40**, 2328–2341 (2020).
14. FAOSTAT (Food and Agriculture Organization of the United Nations, 2020); <http://www.fao.org/faostat/en/#data/QC>
15. *Presidência da República Secretaria-Geral Subchefia para Assuntos Jurídicos* (Ministério da Agricultura, 2015).
16. Rashid, M. A. et al. Impact of heat-wave at high and low VPD on photosynthetic components of wheat and their recovery. *Environ. Exp. Bot.* **147**, 138–146 (2018).
17. Lobell, D. B. et al. Greater sensitivity to drought accompanies maize yield increase in the U.S. Midwest. *Science* **344**, 516–519 (2014).
18. Fletcher, A. L., Sinclair, T. R. & Allen, L. H. Transpiration responses to vapor pressure deficit in well watered 'slow-wilting' and commercial soybean. *Environ. Exp. Bot.* **61**, 145–151 (2007).
19. Bunce, J. A. Comparative responses of leaf conductance to humidity in single attached leaves. *J. Exp. Bot.* **32**, 629–634 (1981).
20. Kiniry, J. et al. Radiation-use efficiency response to vapor pressure deficit for maize and sorghum. *Field Crops Res.* **56**, 265–270 (1998).
21. Spera, S. A. et al. Recent cropping frequency, expansion, and abandonment in Mato Grosso, Brazil had selective land characteristics. *Environ. Res. Lett.* **9**, 064010 (2014).
22. Dias, L. C. P., Pimenta, F. M., Santos, A. B., Costa, M. H. & Ladle, R. J. Patterns of land use, extensification and intensification of Brazilian agriculture. *Glob. Change Biol.* **22**, 2887–2903 (2016).
23. Cohn, A. S., Vanwely, L. K., Spera, S. A. & Mustard, J. F. Cropping frequency and area response to climate variability can exceed yield response. *Nat. Clim. Change* **6**, 601–604 (2016).
24. Morton, D. C. et al. Reevaluating suitability estimates based on dynamics of cropland expansion in the Brazilian Amazon. *Glob. Environ. Change* **37**, 92–101 (2016).
25. Duursma, R. A. et al. The peaked response of transpiration rate to vapour pressure deficit in field conditions can be explained by the temperature optimum of photosynthesis. *Agric. Meteorol.* **189–190**, 2–10 (2014).
26. Spera, S. A., Winter, J. M. & Partridge, T. F. Brazilian maize yields negatively affected by climate after land clearing. *Nat. Sustain.* **3**, 845–852 (2020).
27. Cirino, P. H., Féres, J. G., Braga, M. J. & Reis, E. Assessing the impacts of ENSO-related weather effects on the Brazilian agriculture. *Proc. Econ. Financ.* **24**, 146–155 (2015).
28. Pereira, P. A. A., Martha, G. B., Santana, C. A. & Alves, E. The development of Brazilian agriculture: future technological challenges and opportunities. *Agric. Food Secur.* **1**, 4 (2012).
29. Marengo, J. A. & Bernasconi, M. Regional differences in aridity/drought conditions over Northeast Brazil: present state and future projections. *Climatic Change* **129**, 103–115 (2015).
30. Naylor, R. L. Energy and resource constraints on intensive agricultural production. *Annu. Rev. Energy Environ.* **21**, 99–123 (1996).
31. Getirana, A. Extreme water deficit in Brazil detected from space. *J. Hydrometeorol.* **17**, 591–599 (2016).
32. Lathuilière, M. J., Coe, M. T. & Johnson, M. S. A review of green- and blue-water resources and their trade-offs for future agricultural production in the Amazon Basin: what could irrigated agriculture mean for Amazonia? *Hydrolog. Earth Syst. Sci.* **20**, 2179–2194 (2016).
33. Dobrovolski, R. & Rattis, L. Water collapse in Brazil: the danger of relying on what you neglect. *Nat. Conserv.* **13**, 80–83 (2015).
34. da Silva, A. L. et al. Water appropriation on the agricultural frontier in western Bahia and its contribution to streamflow reduction: revisiting the debate in the Brazilian Cerrado. *Water* **13**, 1054 (2021).
35. Pousa, R. et al. Climate change and intense irrigation growth in western Bahia, Brazil: the urgent need for hydroclimatic monitoring. *Water* **11**, 933 (2019).
36. Ort, D. R. & Long, S. P. Limits on yields in the corn belt. *Science* **344**, 484–485 (2014).
37. de Bossoreille de Ribou, S., Douam, F., Hamant, O., Frohlich, M. W. & Negriotti, I. Plant science and agricultural productivity: why are we hitting the yield ceiling? *Plant Sci.* **210**, 159–176 (2013).
38. Long, S. P. & Ort, D. R. More than taking the heat: crops and global change. *Curr. Opin. Plant Biol.* **13**, 240–247 (2010).
39. Pommer, C. V. & Barbosa, W. The impact of breeding on fruit production in warm climates of Brazil. *Rev. Bras. Frutic.* **31**, 612–634 (2009).
40. Lenka, N. K. et al. Carbon dioxide and temperature elevation effects on crop evapotranspiration and water use efficiency in soybean as affected by different nitrogen levels. *Agric. Water Manag.* **230**, 105936 (2020).
41. Soares, W. R., Marengo, J. A. & Nobre, C. A. Assessment of warming projections and probabilities for Brazil in *Climate Change Risks in Brazil* (eds Nobre, C. et al.) 7–30 (Springer, 2019); https://doi.org/10.1007/978-3-319-92881-4_2
42. Schwalm, C. R., Glendon, S. & Duffy, P. B. RCP8.5 tracks cumulative CO₂ emissions. *Proc. Natl Acad. Sci. USA* **117**, 19656–19657 (2020).
43. Schwalm, C. R., Glendon, S. & Duffy, P. B. Reply to Hausfather and Peters: RCP8.5 is neither problematic nor misleading. *Proc. Natl Acad. Sci. USA* **117**, 27793–27794 (2020).

Publisher's note Springer Nature remains neutral with regard to jurisdictional claims in published maps and institutional affiliations.

© The Author(s), under exclusive licence to Springer Nature Limited 2021

Methods

Our analysis integrates data on changes in crop expansion, productivity, intensification and climate space into a framework for evaluating climate shocks to agriculture. Elucidating the effect of extreme droughts, precipitation, VPD and irrigation on crop yields provides new insights into how climate informs where we decide to grow crops; influences the likelihood of cropland intensification; and may limit crop production in the near future. This approach could be applied elsewhere, given that it relies on remotely sensed data and publicly available databases.

Trends in cropland expansion. The study area spans 2,003,386 km², 68% of which occurs within the Brazilian Legal Amazon—a political designation instituted by the Brazilian government in 1953 to address economic underdevelopment in that part of the country. Approximately 67% of the study area occurs within the Cerrado biome, whereas ~27% occurs in the Amazon biome (the Legal Amazon and the Cerrado biome have a 761,000 km² overlap; Extended Data Fig. 1⁴⁴). Given this geographic complexity, we refer to the study region as the ACR.

We focused our analysis in Brazil because it was the largest soybean producer in the world as recently as 2020⁴⁴. Our specific focus on the states of Mato Grosso, Goiás and the MATOPIBA⁴⁵ region is rooted in four factors: (1) this area alone produces more soybeans than Argentina, the third-largest producer in the world (study area: 64,730,900 t, Argentina: 55,263,891 t)⁴⁴, (2) the region is where most large-scale, export-oriented agriculture occurred over the past five decades, (3) the Brazilian government has ambitious plans to expand agriculture in the region and (4) consistent, accurate and validated crop-specific land-cover maps are available for the entire region^{21,23} (Fig. 1).

To quantify agricultural expansion and contraction, we used published land-use maps for Mato Grosso²¹ and the Cerrado⁸. Those maps classified cropping rotations on the basis of phenological characteristics derived from the Moderate Resolution Imaging Spectroradiometer (MODIS) enhanced vegetation index time series. Three major crops were mapped: soybean, maize and cotton (Supplementary Fig. 3). As of 2016, cotton cultivation was limited to the regions of western Bahia and Mato Grosso under different management systems (Supplementary Fig. 4). Because of differences in growing-season length, rainfed cotton in western Bahia is mostly single cropped. In Mato Grosso, on the other hand, cotton may be cultivated either as a first (single-cropped) or second (following soybean) crop. Altogether, the dataset identifies ten different land uses, but the present study focuses on single-cropped soybeans, single-cropped maize, double-cropped soy/cotton and double-cropped soy/maize because they are the most prevalent and have the longest time series.

We defined agricultural expansion as any area that switched from another use to some combination of soybean, cotton or maize in the target year. We then mapped the expansion of these cultivated areas annually from 2001 to 2016. To quantify changes in planted area over time, we compared the years 2002–2006 to a 2001 baseline, 2007–2011 to 2006 and 2012–2016 to 2011 using the Wilcoxon signed-rank test because the data are not normally distributed. This analysis considered only pixels that were newly converted to agriculture and evaluated climate variables (precipitation, VPD) associated with each.

Drought effects on crop yields. Using a linear mixed model, we evaluated the effects of time, drought and monthly weather condition on agricultural outputs in each state (Cerrado: Maranhão, Tocantins, Piauí, Bahia, Goiás, the Federal District of Brasília; Amazon: Mato Grosso). We then compared soybean and maize yields in time and space as a function of drought and irrigation status.

Agricultural outputs. We gathered the agricultural outputs (for example, planted area, crop yields and total production) of maize second crop and soybeans from the Instituto Brasileiro de Geografia e Estatística (IBGE) database on Municipal Agricultural Production, which synthesizes data from 1974 to 2019. However, soybean data are more consistently available after 1988, and maize first- and second-crop data have been reported separately only since 2003. To account for the positive trend in agricultural outputs, we included years as a random effect in the model. The number of samples in each model varied depending on the number of years that each municipality reported data to the IBGE.

Drought. Using published literature for the Cerrado^{46–48} and the Amazon regions, we first identified the years when climate deviated from the historical mean towards drier and warmer conditions. On the basis of the literature, the Cerrado region faced extreme drought conditions during 1984, 1990, 2007 and 2016, probably due to El Niño phenomena. The Amazon region, on the other hand, had drought events in 1997–1998, 2005, 2010 and 2015^{49–52}. On the basis of drought occurrence, we created a dummy variable (1, drought; 0, normal). We recognize that representing drought as a binary variable may mask heterogeneity in drought occurrence and intensity but our analysis was limited by the fact that crop yield data were available only at the municipal scale. More detailed, spatially explicit data on both the response (crop yield) and predictor (drought occurrence) variables would be preferable. Since these data are currently unavailable, we carefully searched the literature for records of droughts that affected the entire region/biome. Despite these limitations, our analysis detected a response in crop yields. Future studies are needed to identify not only the impact of drought occurrence

and intensity, but also the type and timing of drought impacts on yields and relevant time lags in that response.

Irrigation occurrence. Irrigation occurrence was obtained by the Brazilian Water Agency database⁵. The agency reported the irrigated area in each municipality in 2014 and has updated data to July 2020. To eliminate potentially confounding impacts of irrigation on yield, municipalities where irrigation infrastructure is present were included as an 'irrigated' group and all others in a 'not irrigated' group. The available irrigation data identify only municipalities where some irrigation infrastructure exists, without giving details on when it was installed, the spatial extent or location in the municipality, how much irrigation took place or what crop types are affected. Therefore, the 'irrigated' group should be interpreted as indicating municipalities where some irrigation is possible but not necessarily where it has occurred. The "non-irrigated" group represents those municipalities where irrigation is not taking place and has not impacted yield.

Monthly weather conditions. We evaluated the effect of monthly weather (from September to June) on crop yields for each municipality that grows soybean and maize in the Amazon (Mato Grosso) and Cerrado (Maranhão, Tocantins, Piauí, Bahia and Goiás). We extracted total monthly rainfall from 1981 to 2019 (CHIRPS⁵³: 0.05° latitude × 0.05° longitude) and monthly average VPD from 1981 to 2019 (Terra Climate⁵⁴: 0.04° latitude × 0.04° longitude). We selected these two different sources of climate data given their fine resolution, good data coverage and robustness⁵⁵. We first harmonized the different data resolutions using the functions 'aggregating' and 'resample' available from the raster package in R 3.6.1. Climate data were obtained and pre-processed in the Google Earth Engine Platform⁵⁶, and all the analyses were performed in R⁵⁷.

Whereas precipitation is a measure of water availability, VPD is a measure of aridity calculated on the basis of the difference between the actual air humidity and how much water the air can hold (saturation minus actual water vapour pressure). Changes in the physiological function of the vegetation depend strongly on the atmospheric demand for water, which is driven by VPD and net radiation⁵¹. The VPD increases exponentially as a function of temperature (at constant humidity) and can thus lower water-use efficiency—defined as the amount of biomass (or grain) produced per unit of water¹⁸. By increasing the evaporative potential of the surrounding environment, high VPD can become the dominant driver of water losses from evaporation and transpiration¹⁶. In this context, it is a better surrogate of crop yields than temperature, affecting crop productivity via a variety of mechanisms. A high VPD tends to increase plant transpiration and thereby water demand. Under high soil moisture, this may increase crop yields if extreme conditions are not exceeded. Under low soil moisture, increased transpiration may lead to water stress and negatively impact crop productivity⁵⁸.

Model structure. Crop yields of maize second crop and soybean were modelled separately for the Cerrado and Mato Grosso because of differences in their timing and management. A total of four linear mixed models were built and run using the 'lmer' function in R (package lme4⁵⁹). Response variables were modelled as a function of time, drought occurrence and monthly weather (as fixed terms), whereas municipality ID and year were included as random terms. We started with a global model including all explanatory variables and then selected the best model (using the function 'dredge' in R package MuMin⁶⁰).

Drought effects on agricultural intensification. We analysed the climate conditions associated with specific land-use transitions in the ACR during 2001–2016. Relying on the same crop time series^{8,21}, we applied a two-year temporal filter to identify the following transitions during the study period: (1) single to double cropping (intensification), (2) double to single cropping (de-intensification) and (3) double cropping to fallow (contraction). For each pixel where cropping frequency changed, we extracted the following associated edaphoclimatic variables: precipitation (CHIRPS⁵³), VPD (TerraClimate⁵⁴), onset of the raining season (calculated as described in Arvor⁶¹) and soil characteristics at 0.05 m depth (bulk density, clay and sand content (50–2,000 µm), soil organic carbon content). All physical and chemical soil properties were obtained from the SoilGrids database⁶² (version 0.5.3). Previous analysis has shown that soil texture was not affecting the relative importance of precipitation and VPD, and so we opted to exclude it from this analysis. We have tested two different depth soil layers: 0.05 m and 0.30 m, which has not changed the outcome of the analysis. Also, it is important to highlight that SoilGrids is a statistical product; as such, its variation in depth was found to be small, and the data do not vary substantially between soil layers in the study area⁶³. We then compared the edaphoclimatic properties for each type of transition (intensification, de-intensification and contraction) using a Wilcoxon test ('stat_compare_means' function in R package ggpubr). We also calculated the residence time of double cropping from 2005 to 2016, defined as the total number of years in double cropping (even if not consecutive) divided by the maximum number of years since double-cropping first occurred. All codes and data are available at Zenodo repository⁶⁴.

Changes in double-cropping probability. To calculate the probability of double-cropping occurrence as a function of climate, we first masked out all areas

where double cropping could not occur (for example, water bodies, conservation units, indigenous lands). For remaining areas classified as double cropping, we extracted the total precipitation and mean VPD for the growing season of each year. On the basis of those data, we ran two logistic regressions with a logit link in two models. The first considered the occurrence of double cropping as a function of precipitation, with the year as a co-variable. The second considered double cropping as a function of VPD, with the year as a co-variable. We estimated the parameters for each of the two models and compared them to understand the relative importance of these two key climate variables in cropping decisions.

Changes in climate space in the ACR. The set of climate variables used to define a favourable climate for agriculture delineates an ideal climate space. The WD here is a measure of atmospheric water demand that relates closely to soil moisture and plant water stress. It is most sensitive to changes in temperature, such that increases in temperature cause a large increase in WD. We define climate space as the optimal area for a given land cover/use, adapting the method described by Malhi et al.⁶² and Castanho et al.⁶³. Here, WD is defined as the minimum value of climatological water deficit (CWD) attained during the growing season (September to June), where the monthly change in WD is the difference between precipitation (PPT; mm per month) and evapotranspiration (ET_{rs}; mm per month) for tall crops. For month n

$$\begin{aligned} \text{CWD}_n &= \text{CWD}_{n-1} + \text{PPT}_n - \text{ET}_{rs_n}; \text{Max}(\text{CWD}_n = 0) \\ \text{WD} &= \max(\text{CWD}_{\text{Sept_yr}0}, \dots, \text{CWD}_{\text{June_yr}1}) \end{aligned} \quad (1)$$

For the first month of the growing season, WD_{n-1} was set at zero, so each agricultural year's WD is independent from the previous one. We modelled ET_{rs} calculated on the basis of a Penman–Monteith equation⁶⁴:

$$\text{ET}_{rs} = \frac{0.408 \Delta (R_n - G) + \gamma \frac{C_n}{T+273} u_2 (T_{\min})}{\Delta + \gamma (1 + C_d u_2)} \quad (2)$$

where ET_{rs} is the standardized reference crop evapotranspiration for tall ($>0.5\text{ m}$) crop surfaces (mm per month); R_n is the calculated net radiation at the crop surface (MJ m^{-2} per month); G is the soil heat flux density at the soil surface (MJ m^{-2} per month); T is the mean monthly air temperature ($^{\circ}\text{C}$); and u₂ is the mean wind speed at 2 m height, which was fixed at 3 m s^{-1} . Since data on saturation and mean actual vapour pressure (e_s and e_a) were unavailable, we used the minimum air temperature (T_{\min}) calculated for monthly time steps, as suggested previously⁶⁵. Δ is the slope of the saturation vapour pressure–temperature curve ($\text{kPa}^{\circ}\text{C}^{-1}$); γ is the psychrometric constant ($\text{kPa}^{\circ}\text{C}^{-1}$); C_n is the numerator constant that changes with reference type and time step and C_d is the denominator constant that changes with reference type and time step (s m^{-1}).

To delineate the historical and potential future climate envelopes for the ACR, we summarized the total precipitation during the growing season and WD for all pixels classified as cropland in 2016⁸. Historical and future precipitation during the growing season (1970–2017) were obtained from an ensemble of the 35 global circulation models from the Coupled Model Inter-comparison Project phase 5⁶⁶ (CMIP5), whereas WD was calculated as described above. For the future climatic data, we considered two scenarios, RCP 4.5 W m^{-2} and RCP 8.5 W m^{-2} . CMIP5 seems to be an adequate choice because our temporal scale of assessment is decadal, a scale that CMIP5 has a good accuracy⁶⁹.

Farmers from southern and southeastern Brazil first arrived in the ACR in the 1970s. Although the exact location of agricultural lands at that time is unknown, agricultural expansion in the region has occurred gradually and will probably continue, given continued investments by the region's producers and Brazil's ongoing agricultural policies⁷⁰. Given this, we assume that today's (2016) agricultural fields encompass the areas where the agriculture began in the region. On the basis of the climatic characteristics for soybean, maize and cotton fields in 2016, we drew the minimum convex hull that defines the ideal area for rainfed agriculture. To calculate the effect of historic and potential future climate changes, we considered the relative location of agricultural pixels within climate space, comparing the convex hull of the 1970s with that of the present day and future climate scenarios.

To characterize the relative rate of climate change for each agricultural plot, we calculated the vector of change from one time step to another, considering both the magnitude (speed) and direction of change. The vectors represent the difference in initial and final values for precipitation and WD, thus providing an integrated picture of the combined changes stemming from the two variables. Angles between 181° and 270° represented decreased precipitations and increased dry-season intensity.

Data availability

All the raw climate datasets analysed in this study are available in the Google Earth Engine repository⁵⁶. Raw land-use transition data that support the findings of this section are from published sources^{8,21}. These data were used under license for the current study and are available from the corresponding author upon reasonable request and with permission of S.A.S. (sspera@richmond.edu).

Code availability

Processed and extracted variables used directly in the analyses are available at GitHub (https://github.com/ludmilarattis/effect-of-climate-on--agriculture/tree/Agriculture_Climate). The scripts and datasets used to analyse the effects of climate on agricultural production, land-use transitions and climate space are also available on Zenodo at <https://doi.org/10.5281/zenodo.5363671>.

References

44. *Sistematização das Informações sobre Recursos Naturais—Mapa de Biomas do Brasil* (Instituto Brasileiro de Geografia e Estatística, 2006); <https://www.ibge.gov.br/geociencias/cartas-e-mapas/informacoes-ambientais/15842-biomas.html?=&t=downloads>
45. *Base Cartográfica Contínua Do Brasil, Escala 1:250.000—BC250* (Instituto Brasileiro de Geografia e Estatística, 2019); https://geoftp.ibge.gov.br/cartas_e_mapas/bases_cartograficas_continuas/bc250/versao2019/informacoes_tecnicas/Documentacao_bc250_v2019.pdf
46. Campos, J., de, O. & Chaves, H. M. L. Tendências e variabilidades nas séries históricas da precipitação mensal e anual no bioma Cerrado no período 1977–2010. *Rev. Bras. Meteorol.* **35**, 157–169 (2020).
47. Debortoli, N. S. et al. Rainfall patterns in the southern Amazon: a chronological perspective (1971–2010). *Climatic Change* **132**, 251–264 (2015).
48. Oliveira, P. T. S. et al. Trends in water balance components across the Brazilian Cerrado. *Water Resour. Res.* **50**, 7100–7114 (2014).
49. Panisset, J. S. et al. Contrasting patterns of the extreme drought episodes of 2005, 2010 and 2015 in the Amazon Basin. *Int. J. Climatol.* **38**, 1096–1104 (2018).
50. Cai, W. et al. Increasing frequency of extreme El Niño events due to greenhouse warming. *Nat. Clim. Change* **4**, 111–116 (2014).
51. Jiménez-Muñoz, J. C. et al. Record-breaking warming and extreme drought in the Amazon rainforest during the course of El Niño 2015–2016. *Sci. Rep.* **6**, 33130 (2016).
52. Marengo, J. A. & Espinoza, J. C. Extreme seasonal droughts and floods in Amazonia: causes, trends and impacts. *Int. J. Climatol.* **36**, 1033–1050 (2016).
53. Funk, C. et al. The climate hazards infrared precipitation with stations—a new environmental record for monitoring extremes. *Sci. Data* **2**, 150066 (2015).
54. Abatzoglou, J. T., Dobrowski, S. Z., Parks, S. A. & Hegewisch, K. C. TerraClimate, a high-resolution global dataset of monthly climate and climatic water balance from 1958–2015. *Sci. Data* **5**, 170191 (2018).
55. Harris, I., Osborn, T. J., Jones, P. & Lister, D. Version 4 of the CRU TS monthly high-resolution gridded multivariate climate dataset. *Sci. Data* **7**, 109 (2020).
56. Gorelick, N. et al. Google Earth Engine: planetary-scale geospatial analysis for everyone. *Remote Sens. Environ.* **202**, 18–27 (2017).
57. R Core Team *R: A Language and Environment for Statistical Computing* (R Foundation for Statistical Computing, 2019).
58. Challinor, A. J. & Wheeler, T. R. Crop yield reduction in the tropics under climate change: processes and uncertainties. *Agric. Meteorol.* **148**, 343–356 (2008).
59. Bates, D. et al. *lme4*. R package version (2012).
60. Barton, K. *MuMin*: Multi-model inference. R package version 1.0.0 (2009).
61. Arvor, D., Dubreuil, V., Ronchail, J., Simões, M. & Funatsu, B. M. Spatial patterns of rainfall regimes related to levels of double cropping agriculture systems in Mato Grosso (Brazil). *Int. J. Climatol.* **34**, 2622–2633 (2014).
62. Hengl, T. et al. SoilGrids250m: global gridded soil information based on machine learning. *PLoS ONE* **12**, e0169748 (2017).
63. Brill, F., Passuni Pineda, S., Espichán Cuya, B. & Kreibich, H. A data-mining approach towards damage modelling for El Niño events in Peru. *Geomat. Nat. Hazards Risk* **11**, 1966–1990 (2020).
64. Rattis, L. *ludmilarattis/effect-of-climate-on--agriculture: Rattis_etal_NCC_2021*. Zenodo <https://zenodo.org/badge/latestdoi/271879616> (2021).
65. Malhi, Y. et al. Exploring the likelihood and mechanism of a climate-change-induced dieback of the Amazon rainforest. *Proc. Natl Acad. Sci. USA* **106**, 20610–20615 (2009).
66. Castanho, A. D. A. et al. Potential shifts in the aboveground biomass and physiognomy of a seasonally dry tropical forest in a changing climate. *Environ. Res. Lett.* **15**, 034053 (2020).
67. Allen, R. G. et al. *The ASCE Standardized Reference Evapotranspiration Equation* (American Society of Civil Engineers, 2005).
68. *IPCC Climate Change 2014: Synthesis Report* (eds Core Writing Team, Pachauri, R. K. & Meyer, L. A.) (IPCC, 2014).
69. Koutroulis, A. G., Grillakis, M. G., Tsanis, I. K. & Papadimitriou, L. Evaluation of precipitation and temperature simulation performance of the CMIP3 and CMIP5 historical experiments. *Clim. Dyn.* **47**, 1881–1898 (2016).
70. *Análise Territorial para o Desenvolvimento da Agricultura Irrigada no Brasil* (Ministério da Integração Nacional, 2014).

Acknowledgements

This work was supported through funding from the NSF INFEWS/T1 (#1739724), CNPq/ANA (#446412/2015-5), MCTIC/CNPq – NEXUS 19/2017 (#441463/2017-7) and CNPq/PELD (#441703/2016-0). We thank B. Rebelatto, A. Ribeiro, N. Muller and S. Davis for discussions and P. Lefebvre and C. Churchill for advice in mapping techniques. We also acknowledge that the study area encompasses the traditional land of Indigenous people of more than 80 different ethnicities.

Author contributions

L.R., P.M.B., M.N.M. and M.T.C. conceived of the presented ideas and wrote the manuscript; S.A.S. investigated the land-use transition patterns and helped to revise the findings of this work. L.R. performed the analytic calculations with support from A.D.A.C., N.Q.C., E.Q.M. and D.V.S. All authors contributed in the final version of the manuscript.

Competing interests

The authors declare no competing interests.

Additional information

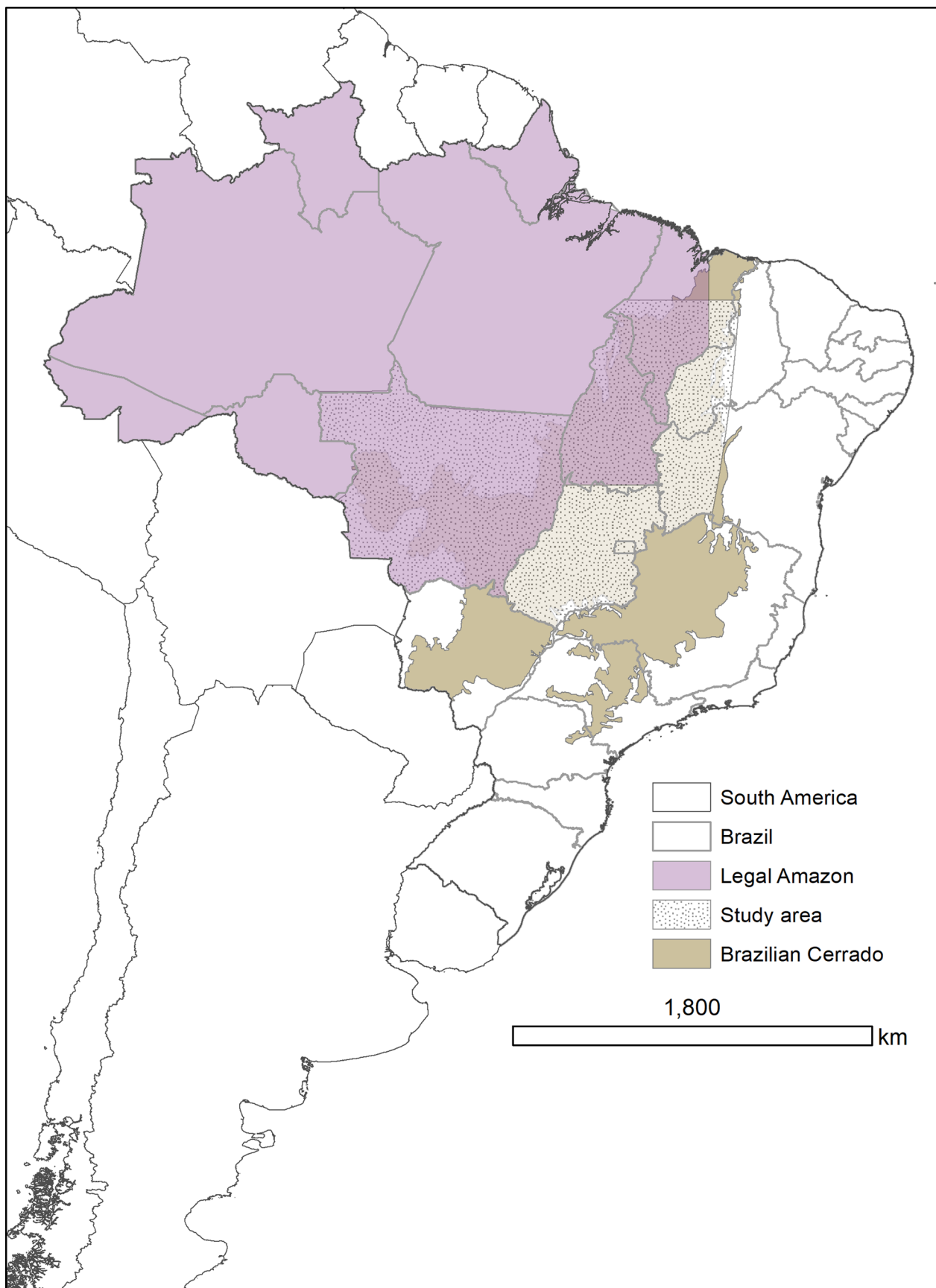
Extended data is available for this paper at <https://doi.org/10.1038/s41558-021-01214-3>.

Supplementary information The online version contains supplementary material available at <https://doi.org/10.1038/s41558-021-01214-3>.

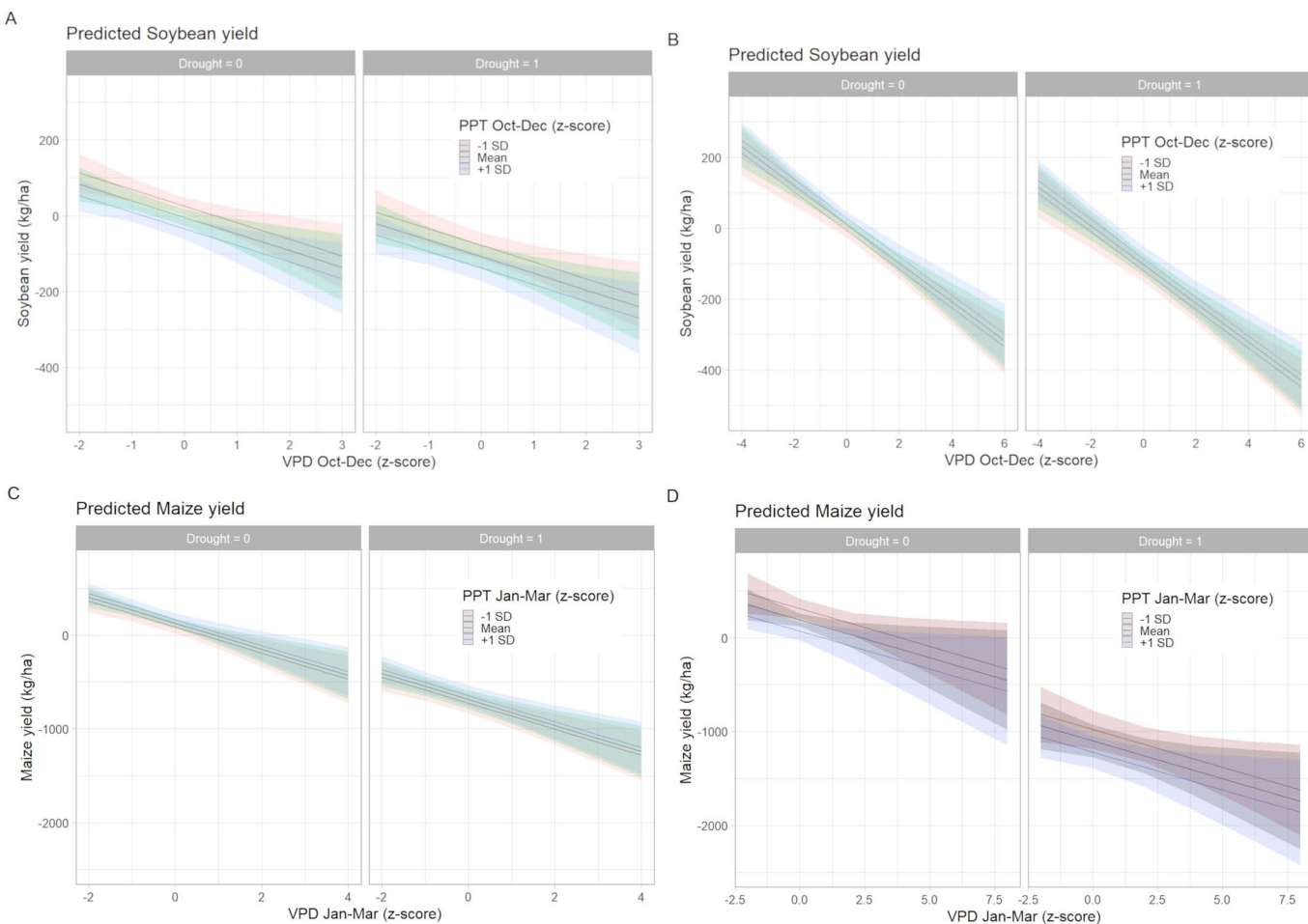
Correspondence and requests for materials should be addressed to Ludmila Rattis.

Peer review information *Nature Climate Change* thanks Marcelo Galdos, Guiling Wang, Anita Wreford and the other, anonymous, reviewer(s) for their contribution to the peer review of this work.

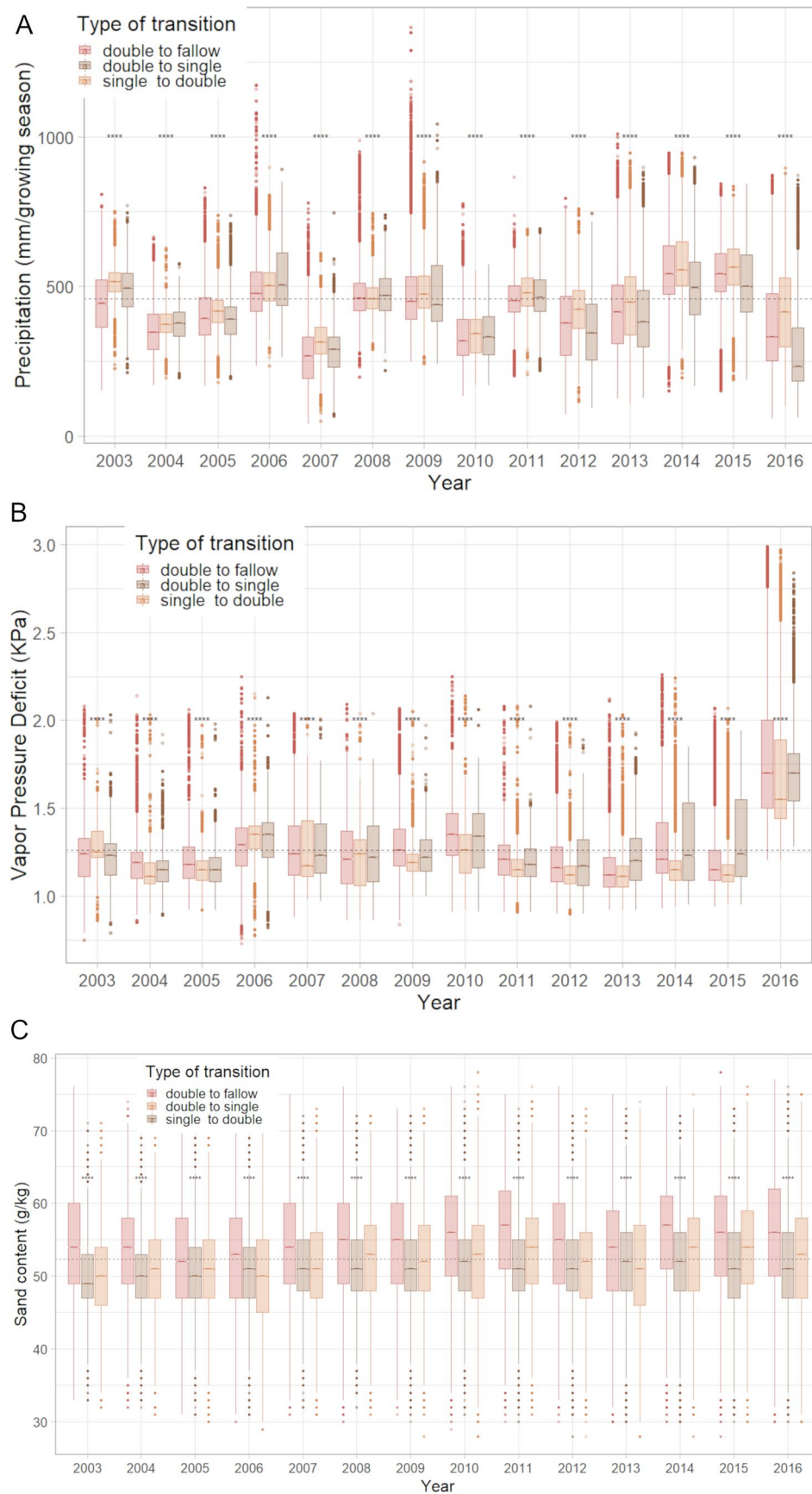
Reprints and permissions information is available at www.nature.com/reprints.



Extended Data Fig. 1 | Location of the study area relative to Brazilian biomes. The study region location relative to the Legal Amazon and Cerrado biome. Approximately 68% of the study region falls within the Legal Amazon. The region spans the Cerrado (67.2%), Amazon (~27%) (the Legal Amazon and the Cerrado biome have a 761 km² overlap), Pantanal (3.2%), Caatinga (1.7%), and Atlantic Forest (1.3%) biomes.

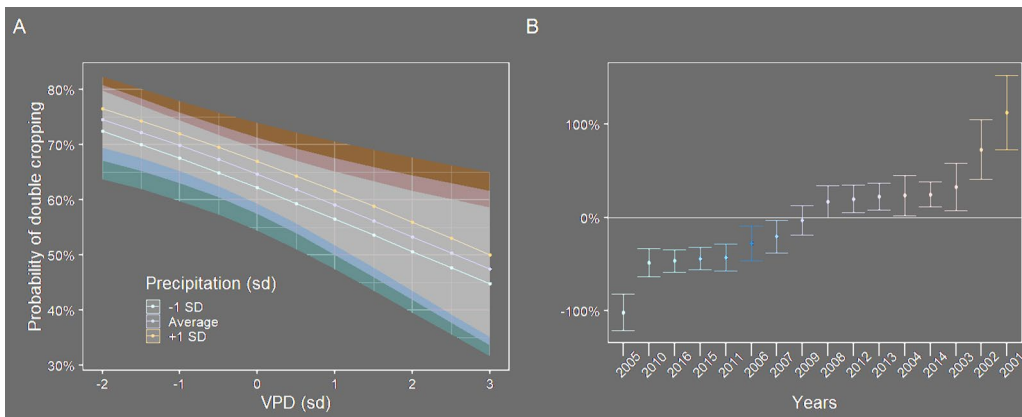


Extended Data Fig. 2 | Predicting crop yields as a function of monthly weather conditions. Soybean and maize second crop yields as a function of precipitation and vapor pressure deficit at early stages of development. We predicted soybean (A B) and maize second crop yields as a function of VPD and precipitation in Mato Grosso (A and C) and Cerrado (B and D). The effects of monthly weather were tested in drought (on the left of each panel) and in non-drought (on the right of each panel) conditions.

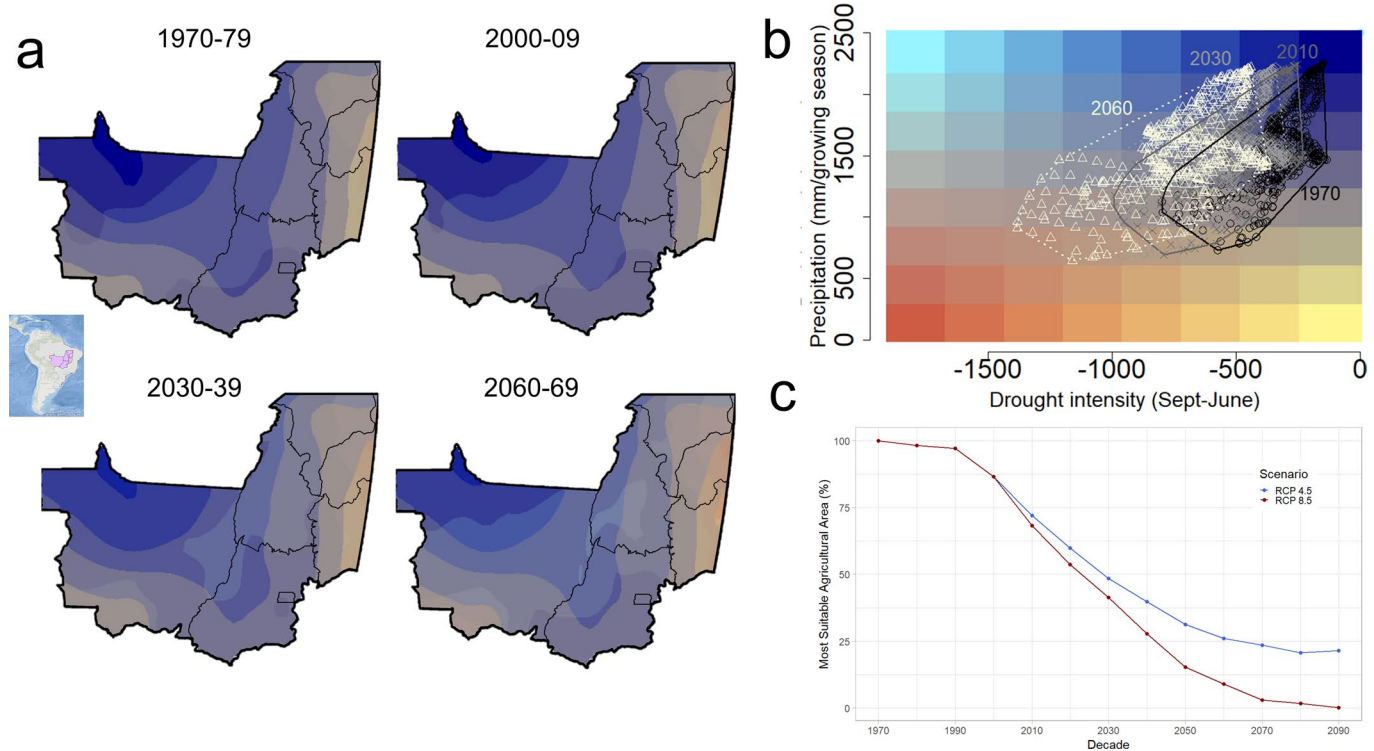


Extended Data Fig. 3 | See next page for caption.

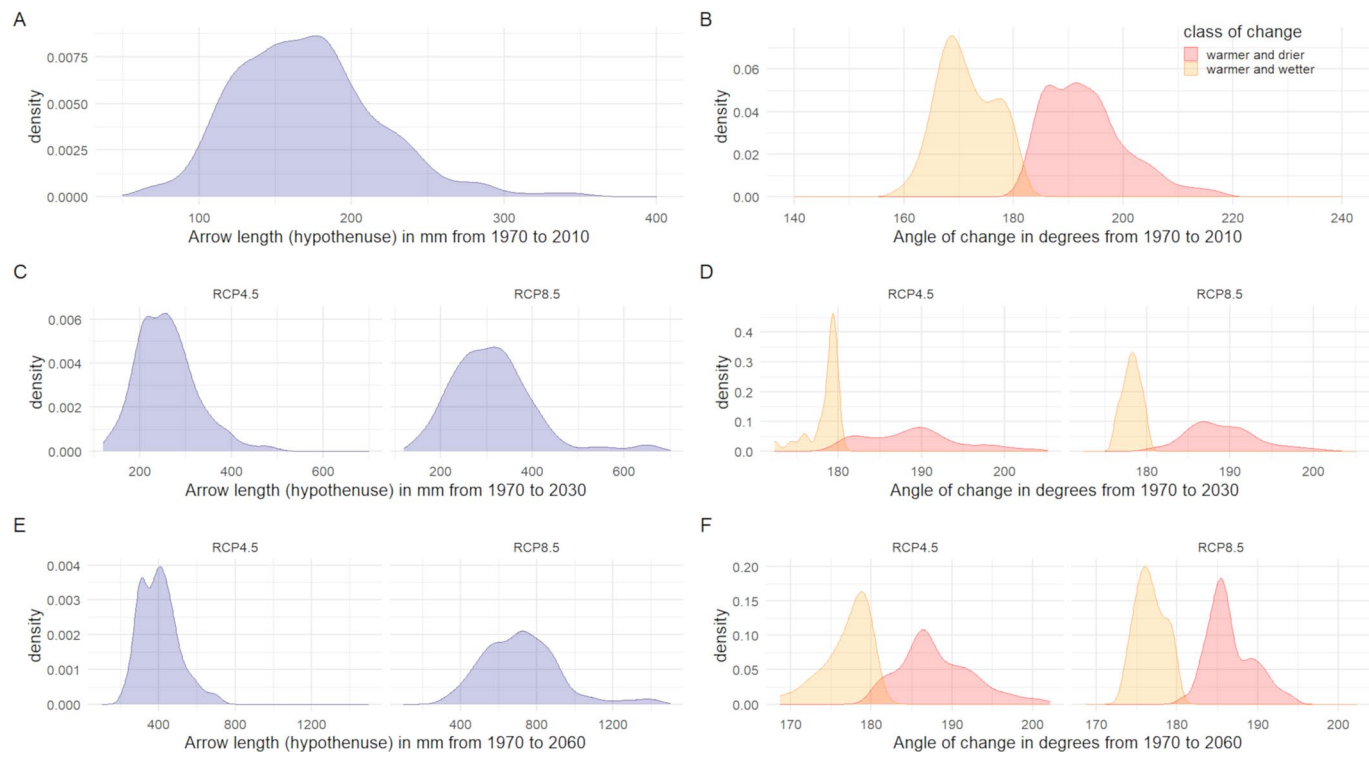
Extended Data Fig. 3 | Edaphoclimatic conditions in areas where the agriculture has either intensified and de-intensified. Edaphoclimatic conditions in areas where the agriculture has either intensified and de-intensified. Precipitation (A), VPD (B) and Sand Content (C) of the growing season. In red, double-cropping to fallowing; in brown, double- to single-cropping and in orange, from single- to double-cropping. Only transitions with a consistency of two years were considered. We have tested if the groups presented differences among their means using Kruskal-Wallis test and present it for each year.



Extended Data Fig. 4 | Predicting double-cropping occurrence as a function of monthly weather conditions. Predicted values of changes in double-cropping occurrence as a function of A) the observed precipitation and VPD, B) using year as a random term in the agricultural plots from 2002 to 2016. For each 100 mm decrease in the total precipitation the chances of double-cropping decreased by 2%. For each 1KPa increase in VPD, the chances of double cropping decreased by 30%.



Extended Data Fig. 5 | Climate envelope for the Amazon Cerrado region according to RCP 4.5 W/m. The climate envelope for the last 50 years in the Amazon Cerrado Region based on past observed data: 1970–1979 (solid line in black); 2000–2009 (solid line in pink); and on future modeled data (CMIP5–RCP 4.5 W m⁻²): 2020–2029 (dotted line in salmon) and 2060–2069 (dotted line in purple). Each pixel on the maps (on the left) correspond to one point in the scatterplot (on the right). The colors on map are the same as the point falls on the background of the scatter plot. The convex hulls delimit the climate conditions in the represented decade.



Extended Data Fig. 6 | Magnitude of change of climatic conditions of each agricultural plot in the Amazon Cerrado Region. Quantifying the magnitude of change of climatic conditions of each agricultural plot in the Amazon Cerrado Region. Panels A, C and E show the distribution of distance in mm each agricultural plot had changed from 1970 to 2010 (A), from 1970 to 2030 (C) and from 1970 to 2060 (E). The direction of those changes are shown in panels B (1970–2010), D (1970–2030) and F (1970–2060). All agricultural plots became warmer. In yellow those moving to warmer and wetter conditions. In red those moving towards warmer and drier conditions. one point in the scatterplot (on the right).